

Bounding the Higgs Boson Width Through Interferometry

Lance J. Dixon¹ and Ye Li¹

¹*SLAC National Accelerator Laboratory, Stanford University, Stanford, CA 94309, USA*

We study the change in the di-photon invariant mass distribution for Higgs boson decays to two photons, due to interference between the Higgs resonance in gluon fusion and the continuum background amplitude for $gg \rightarrow \gamma\gamma$. Previously, the apparent Higgs mass was found to shift by around 100 MeV in the Standard Model in the leading order approximation, which may potentially be experimentally observable. We compute the next-to-leading order QCD corrections to the apparent mass shift, which reduce it by about 40%. The apparent mass shift may provide a way to measure, or at least bound, the Higgs boson width at the Large Hadron Collider through “interferometry”. We investigate how the shift depends on the Higgs width, in a model that maintains constant Higgs boson signal yields. At Higgs widths above 30 MeV the mass shift is over 200 MeV and increases almost linearly with the width. The apparent mass shift could be measured by comparing with the ZZ^* channel, where the shift is much smaller. It might be possible to measure the shift more accurately by exploiting its strong dependence on the Higgs transverse momentum.

INTRODUCTION

Recently, experiments at the Large Hadron Collider (LHC) have discovered a new boson with a mass around 125 GeV [1, 2], whose properties are roughly consistent with those predicted for the Standard Model (SM) Higgs boson. It is now crucial to determine its properties as accurately as possible. The Higgs boson is dominantly produced by gluon fusion through a top quark loop. Its decay to two photons, $H \rightarrow \gamma\gamma$, provides a very clean signature for probing Higgs properties, including its mass. However, there is also a large continuum background to its detection in this channel. It is important to study how much the coherent interference between the Higgs signal and the background could affect distributions in diphoton observables, and possibly use it to constrain Higgs properties.

The interference of the Higgs boson with $gg \rightarrow \gamma\gamma$ was first studied for an intermediate Higgs mass boson [3]. For the experimentally relevant case of a light, narrow-width Higgs boson, it is fruitful to divide the interference contribution into two parts, proportional to the real and imaginary part of the Higgs boson’s Breit-Wigner propagator, respectively. The diphoton invariant-mass distribution for the real-part interference is odd around the Higgs mass. It contributes negligibly to the experimentally observed cross section, which is integrated over the narrow lineshape. The imaginary part interferes constructively or destructively with the signal distribution at the Higgs mass. For a light SM Higgs boson, the imaginary part vanishes at leading order in the zero quark mass limit [3]. The dominant contribution comes from the two-loop $gg \rightarrow \gamma\gamma$ amplitude and gives only a few percent suppression of the rate [4]. However, the real part interference is affected by finite detector resolution, which smears the diphoton invariant mass distribution and causes a sizable shift in the apparent Higgs mass peak, as pointed out in ref. [5] and further studied in refs. [6, 7].

In this letter, we calculate the dominant next-to-leading order (NLO) QCD corrections to the interference, and study the dependence of the mass shift on the acceptance cuts. We further argue that the interference effect, especially the mass shift, can be used to bound experimentally, or possibly even measure, the Higgs width fairly directly, for widths well below the experimental mass resolution at the LHC. Such a measurement would complement even more direct measurements of the Higgs width at future colliders such as the ILC [8, 9] or a muon collider [10, 11], but might be accomplished much earlier.

Indirect bounds on the Higgs width at LHC have also been given based on global analyses of various Higgs decay channels [12–14]. However, in these analyses it is impossible to decouple the Higgs width from the couplings without a further assumption, because the Higgs signal strength is always given by the product of squared couplings for Higgs production and for decay, divided by the Higgs total width Γ_H . Typically the further assumption is that the Higgs coupling to electroweak vector bosons does not exceed the SM value. For example, a recent CMS analysis making this assumption obtained a 95% confidence level upper limit on the beyond-SM width of the Higgs boson of $0.64\Gamma_H$, corresponding to $\Gamma_H/\Gamma_H^{SM} < 2.8$ [14]. Also, a Higgs width dominated by invisible modes can be ruled out by direct search [15]. We demonstrate here that the interference effect, because of its different dependence on the Higgs width, allows Γ_H to be constrained independently of assumptions about couplings or new decay modes.

THEORETICAL DESCRIPTION

The NLO QCD formulae for Higgs production via gluon fusion are well known [16]. The SM continuum background for gluon fusion into two photons is also known at NLO [17]. (As a component of the inclusive diphoton background, $pp \rightarrow \gamma\gamma X$, the process $gg \rightarrow \gamma\gamma$

technically begins at NNLO, but it is greatly enhanced by the large gluon parton distribution function (PDF) at small x .) Here we present the dominant NLO corrections to the interference between the Higgs signal and background in QCD.

Figure 1 shows, first, the leading-order contribution to the interference [denoted by LO (gg)] of the resonant amplitude $gg \rightarrow H \rightarrow \gamma\gamma$ with the one-loop continuum $gg \rightarrow \gamma\gamma$ amplitude mediated by the five light quark flavors. We also include the tree-level process $q\bar{q} \rightarrow \gamma\gamma$, whose interference with $q\bar{q} \rightarrow Hq \rightarrow \gamma\gamma q$ [denoted by LO ($q\bar{q}$)] is at the same order in α_s as the leading $gg \rightarrow H \rightarrow \gamma\gamma$ interference, although suppressed by the smaller quark PDF. It was already considered in refs. [6, 7]. The contribution from $q\bar{q} \rightarrow Hg \rightarrow \gamma\gamma g$ is numerically tiny [6, 7] and we will neglect it.

Finally, fig. 1 depicts the three types of continuum amplitudes mediated by light quark loops that we include in the dominant NLO corrections [denoted by NLO (gg)]: the real radiation processes, $gg \rightarrow \gamma\gamma g$ and $q\bar{q} \rightarrow \gamma\gamma q$ at one loop, and the virtual two-loop $gg \rightarrow \gamma\gamma$ process. All these amplitudes are adapted from refs. [18–20]. The soft and collinear divergences in the real radiation process are handled by dipole subtraction [21, 22]. Although the contribution from $q\bar{q} \rightarrow \gamma\gamma q$ via a light quark loop is not the complete contribution to this amplitude, it forms a gauge-invariant subset and it is enhanced by a sum over quark flavors, so that it gives a significant contribution to the interference at finite Higgs transverse momentum.

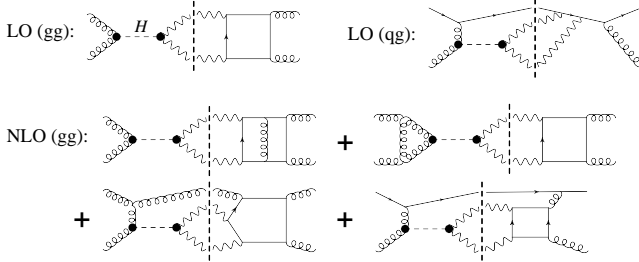


FIG. 1. Representative diagrams for interference between the Higgs resonance and the continuum in the diphoton channel. The dashed vertical lines separate the resonant amplitudes from the continuum ones.

In order to parametrize possible deviations from the SM in the coupling of the Higgs boson to the massless vector boson pairs gg and $\gamma\gamma$, we adopt the notation of ref. [23] for the effective Lagrangian,

$$\mathcal{L} = - \left[\frac{\alpha_s}{8\pi} c_g b_g G_{a,\mu\nu} G_a^{\mu\nu} + \frac{\alpha}{8\pi} c_\gamma b_\gamma F_{\mu\nu} F^{\mu\nu} \right] \frac{h}{v}, \quad (1)$$

where $b_{g,\gamma}$ are defined to absorb all SM contributions and $c_{g,\gamma}$ differ from 1 in the case of new physics. The lineshape for the Higgs boson can be divided into a pure signal term and an interference correction, which we write

schematically in the narrow-width approximation (NWA) as,

$$\frac{d\sigma^{sig}}{dM_{\gamma\gamma}} = \frac{S}{(M_{\gamma\gamma}^2 - m_H^2)^2 + m_H^2 \Gamma_H^2}, \quad (2)$$

$$\frac{d\sigma^{int}}{dM_{\gamma\gamma}} = \frac{(M_{\gamma\gamma}^2 - m_H^2)R + m_H \Gamma_H I}{(M_{\gamma\gamma}^2 - m_H^2)^2 + m_H^2 \Gamma_H^2}. \quad (3)$$

The signal factor S is proportional to $c_g^2 c_\gamma^2$, while the real and imaginary parts of the interference terms, R and I , are proportional to $c_g c_\gamma$. We take the resonance mass to be $m_H = 125$ GeV and the SM value of the width to be $\Gamma_H^{SM} = 4$ MeV [24]. In the NWA, the integral of the cross section over the resonance is given by $\pi S / (2m_H^2 \Gamma_H)$ and $\pi I / (2m_H)$ for signal and interference respectively. An important feature is that the integrated interference contribution has a different dependence on the Higgs width and couplings than does the signal, *i.e.* $c_g c_\gamma$ vs. $c_g^2 c_\gamma^2 / \Gamma_H$. Hence it could potentially be used to constrain Γ_H independently of the Higgs couplings.

The theoretical lineshapes (2) and (3) are very narrow, and strongly broadened by the experimental resolution. The main effect of the real term R after this broadening is to shift the apparent mass slightly [5]. Following ref. [5], we model the experimental resolution by a Gaussian distribution. Although a definitive study of the apparent mass shift has to be performed by the experimental collaborations, using a complete description of the resolution and the background model, we estimate it as follows: For the distribution in a given variable, for example the diphoton invariant mass M , the likelihood of obtaining N events with $M = M_1, M_2, \dots, M_N$ is given by,

$$L = \frac{\mathcal{L}^N}{N!} e^{-\tilde{N}} \prod_{i=1}^N \left. \frac{d\tilde{\sigma}}{dM} \right|_{M=M_i}, \quad (4)$$

where \mathcal{L} is the integrated luminosity. Variables with tildes denote the prediction of the “experimental model”, a pure Gaussian with a variable mass parameter \tilde{m}_H . For the true distribution, obtained by convoluting the sum of eqs. (2) and (3) with a Gaussian of the same width, $\sigma = 1.7$ GeV, we use variables without tildes. To fit for the shifted mass, we minimize the test statistic $t = -2 \ln L$ with respect to \tilde{m}_H . We derived the following equation determining the mass shift $\Delta m_H \equiv \tilde{m}_H - m_H$:

$$0 = \delta \langle t \rangle \propto \int dM \frac{\frac{d\tilde{\sigma}}{dM} - \frac{d\sigma}{dM}}{\frac{d\tilde{\sigma}}{dM}} \delta \frac{d\tilde{\sigma}}{dM} \approx \int dM \frac{\frac{d\tilde{\sigma}}{dM} - \frac{d\sigma}{dM}}{\frac{d\tilde{\sigma}}{dM}} \delta \frac{d\tilde{\sigma}}{dM} = \delta \left[\int dM \frac{\left(\frac{d\tilde{\sigma}}{dM} - \frac{d\sigma}{dM} \right)^2}{2 \frac{d\tilde{\sigma}}{dM}} \right] \quad (5)$$

where $\delta \equiv \delta / \delta \tilde{m}_H$. Because $\frac{d\sigma}{dM}$ in the denominator should include the large continuum background, which is roughly constant throughout the range of consideration, eq. (5) reduces to a simple least-squares fit. The mass

shift obtained from this fit is stable once we include invariant masses ranging out to three times the Gaussian width. (In practice we performed a fit varying the height and width of the Gaussian as well as the mass; however, the former two quantities are hardly affected by the real part of the interference.)

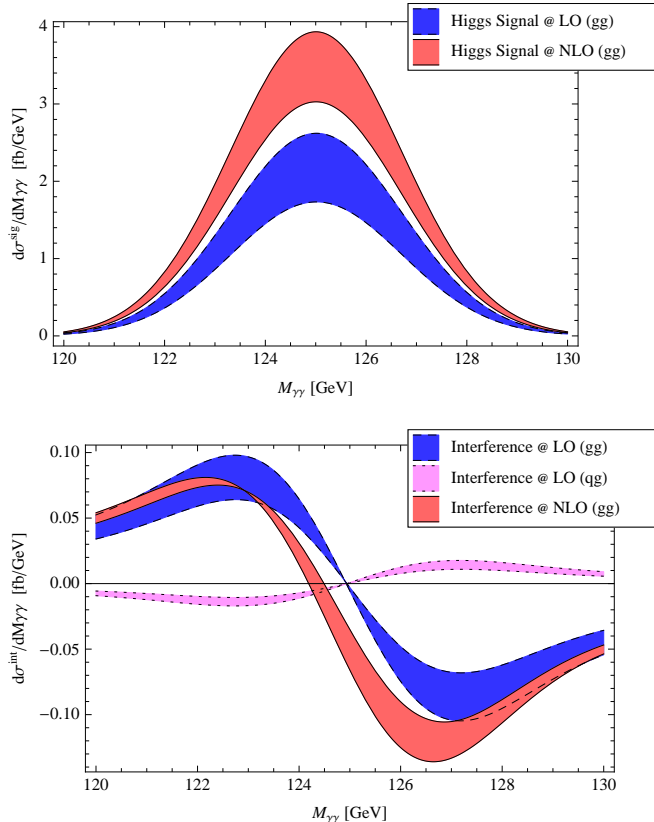


FIG. 2. Diphoton invariant mass $M_{\gamma\gamma}$ distribution for pure signal (top panel) and interference term (bottom panel) after Gaussian smearing.

The top panel of fig. 2 shows the Gaussian-smearred diphoton invariant mass distribution for the pure signal at both LO and NLO in QCD. We use the MSTW2008 NLO PDF set and α_s [25] throughout, and set $\alpha = 1/137$. Standard acceptance cuts are applied to the photon transverse momenta, $p_{T,\gamma}^{\text{hard/soft}} > 40/30$ GeV, and rapidities, $|\eta_\gamma| < 2.5$. In addition, events are discarded when a jet with $p_{T,j} > 3$ GeV is within $\Delta R_{\gamma j} < 0.4$ of a photon. A jet veto is simulated by throwing away events with $p_{T,j} > 20$ GeV and $\eta_j < 3$. The scale uncertainty bands are obtained by varying $m_H/2 < \mu_F, \mu_R < 2m_H$ independently. Note that the NLO (gg) channel includes the contribution from the qq channel where the quark splits to a gluon; this reduces dependence on the factorization scale μ_F . As a result, the scale uncertainty bands mostly come from varying the renormalization scale μ_R .

The bottom panel of fig. 2 shows the corresponding Gaussian-smearred interference contributions. The contribution involving the SM tree amplitude for $qq \rightarrow \gamma\gamma q$ is denoted by LO (qq). The destructive interference from the imaginary part I in eq. (3) shows up at two-loop order in the gluon channel in the zero mass limit of light quarks [4]. It produces the offset of the NLO (gg) curve from zero at $M_{\gamma\gamma} = 125$ GeV.

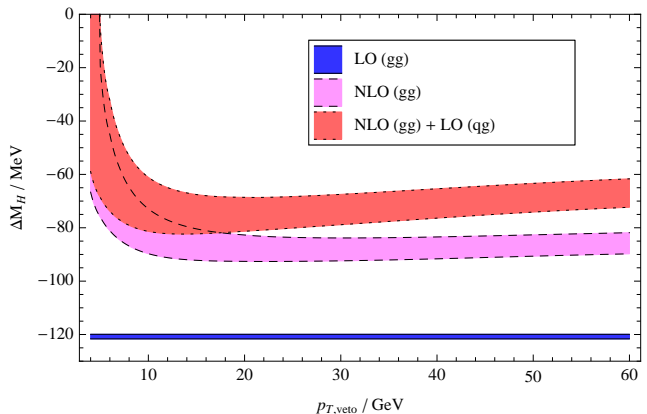


FIG. 3. Apparent mass shift for SM Higgs versus jet veto p_T .

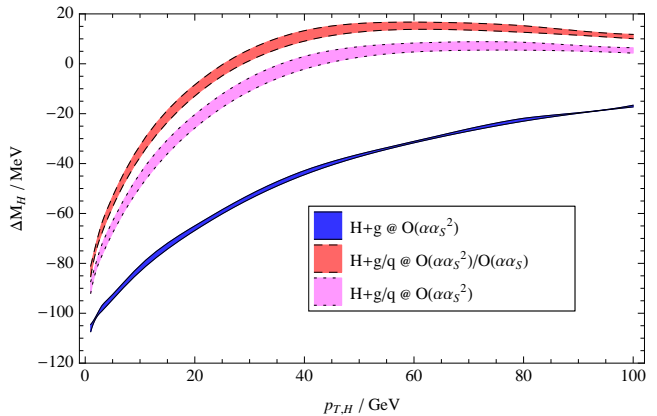


FIG. 4. Apparent mass shift for SM Higgs versus Higgs p_T .

THE MASS SHIFT

In fig. 3 we plot the dependence of the apparent Higgs boson mass shift, as a function of the jet veto p_T cut. The mass shift for inclusive production (large $p_{T,\text{veto}}$) is found to be around 70 MeV at NLO. This is significantly smaller than the prediction of 120 MeV at LO, mainly due to the large NLO QCD Higgs production K factor. The K factor for the SM continuum background is also sizable due to the same gluon incoming states. But the

Higgs signal receives an additional enhancement from the virtual correction to the top quark loop, which is missing in the continuum background [17]. As expected, the K factor of the interference is between that of the signal and background, if we neglect the new destructive interference starting at two loops. For moderate jet veto cuts, the mass shift has a very weak dependence on p_T due to the smallness of the real radiation contribution. The extra interference with quark-gluon scattering at tree level results in a small additional reduction in the mass shift, as shown in the curve labeled NLO (gg) + LO (qg) in fig. 3. At small veto p_T , the results become unreliable: large logarithms spoil the convergence of perturbation theory, and resummation is required, which is beyond the scope of this letter.

In fig. 4 we study how the mass shift depends on the Higgs transverse momentum $p_{T,H}$. This strong dependence could potentially be observed experimentally, completely within the $\gamma\gamma$ channel, without having to compare against a mass measurement using the only other high-precision channel, ZZ^* . (The mass shift for ZZ^* is much smaller than for $\gamma\gamma$, as can be inferred from fig. 17 of ref. [26], because $H \rightarrow ZZ^*$ is a tree-level decay, while the continuum background $gg \rightarrow ZZ^*$ arises at one loop, the same order as $gg \rightarrow \gamma\gamma$.) Using only $\gamma\gamma$ events might lead to reduced experimental systematics associated with the absolute photon energy scale. The $p_{T,H}$ dependence of the mass shift was first studied in ref. [7]. The dotted magenta band includes, in addition, the continuum process $qg \rightarrow \gamma\gamma q$ at one loop via a light quark loop, a part of the full $\mathcal{O}(\alpha_s^2)$ correction. This new contribution partially cancels against the tree-level qg channel, leading to a larger negative Higgs mass shift. The scale variation of the mass shift at finite $p_{T,H}$ is very small, because it is essentially a LO analysis; the scale variation largely cancels in the ratio between interference and signal that enters the mass shift.

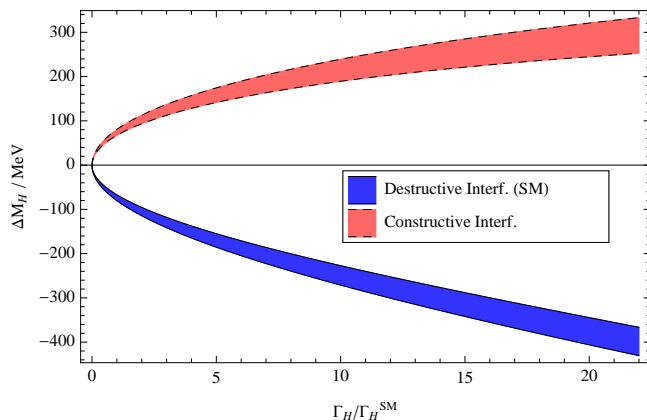


FIG. 5. Higgs mass shift as a function of the Higgs width. The coupling $c_{g\gamma}$ has been adjusted to maintain a constant signal yield.

Finally, we allow the Higgs width to differ from the SM prediction. The Higgs couplings to gluons, photons, and other observed final states should then change accordingly, in order to maintain roughly SM signal yields, as is in reasonable agreement with current LHC measurements. In particular, for the product $c_g c_\gamma = c_{g\gamma}$ entering the dominant gluon fusion contribution to the $\gamma\gamma$ yield, we solve the following equation,

$$\frac{c_{g\gamma}^2 S}{\Gamma_H} + c_{g\gamma} I = \frac{S}{\Gamma_H^{SM}} + I. \quad (6)$$

The mass shift is directly proportional to $c_{g\gamma}$. On the right-hand side of eq. (6), the two-loop imaginary interference term I is negligible; the fractional destructive interference in the SM is $I \Gamma_H^{SM} / S \approx -1.6\%$. When I can also be neglected on the left-hand side, the solution for $c_{g\gamma}$ is simply $c_{g\gamma} = \sqrt{\Gamma_H / \Gamma_H^{SM}}$. Fig. 5 shows that the mass shift is indeed proportional to $\sqrt{\Gamma_H}$ for small Higgs widths. However, once the width Γ_H exceeds several times the SM width, the term $c_{g\gamma} I$ becomes significant on the left-hand side of eq. (6). Then $c_{g\gamma}$ increases more rapidly, almost linearly with Γ_H , assuming the same sign (destructive) interference as in the SM. If new physics somehow reversed the sign of the Higgs diphoton amplitude, one would obtain a constructive interference and a positive mass shift instead. In this case, also shown in fig. 5, the mass shift flattens out at large Γ_H .

DISCUSSION

In this letter, we have studied the interference of a SM Higgs boson with the LHC diphoton continuum background at NLO in QCD. The mass shift is largely stable for moderate jet veto p_T cuts. In addition, we provide a slightly more precise prediction for the mass shift at finite Higgs p_T , by including the contribution from quark-gluon scattering via quark loops. The strong p_T -dependence of the mass shift may allow its measurement without reference to the ZZ^* channel. Furthermore, we consider a scenario in which new physics modifies the Higgs width without altering event rates in the diphoton channel. The mass shift increases rapidly with the Higgs width, which could potentially lead to a more direct bound on the Higgs width than is presently available.

ACKNOWLEDGMENT

We are grateful to Glen Cowan, Daniel de Florian, Louis Fayard, Tom Junk, Steve Martin and Reisaburo Tanaka for helpful comments. We thank Stefan H"ocher for useful discussions and help with the numerical implementation. This research was supported by the US Department of Energy under contract DE-AC02-76SF00515.

-
- [1] S. Chatrchyan *et al.* [CMS Collaboration], Phys. Lett. B **716**, 30 (2012) [arXiv:1207.7235 [hep-ex]].
- [2] G. Aad *et al.* [ATLAS Collaboration], Phys. Lett. B **716**, 1 (2012) [arXiv:1207.7214 [hep-ex]].
- [3] D. A. Dicus and S. S. D. Willenbrock, Phys. Rev. D **37**, 1801 (1988).
- [4] L. J. Dixon and M. S. Siu, Phys. Rev. Lett. **90**, 252001 (2003) [hep-ph/0302233].
- [5] S. P. Martin, Phys. Rev. D **86**, 073016 (2012) [arXiv:1208.1533 [hep-ph]].
- [6] D. de Florian, N. Fidanza, R. J. Hernández-Pinto, J. Mazzitelli, Y. R. Habarnau and G. F. R. Sborlini, arXiv:1303.1397 [hep-ph].
- [7] S. P. Martin, arXiv:1303.3342 [hep-ph].
- [8] F. Richard and P. Bambade, hep-ph/0703173 [HEP-PH].
- [9] M. E. Peskin, arXiv:1207.2516 [hep-ph].
- [10] T. Han and Z. Liu, Phys. Rev. D **87**, 033007 (2013) [arXiv:1210.7803 [hep-ph]].
- [11] A. Conway and H. Wenzel, arXiv:1304.5270 [hep-ex].
- [12] B. A. Dobrescu and J. D. Lykken, JHEP **1302**, 073 (2013) [arXiv:1210.3342 [hep-ph]].
- [13] A. Djouadi and G. Moreau, arXiv:1303.6591 [hep-ph].
- [14] S. Chatrchyan *et al.* [CMS Collaboration], CMS PAS HIG-13-005 (2013), unpublished.
- [15] G. Aad *et al.* [ATLAS Collaboration], ATLAS-CONF-2013-011.
- [16] A. Djouadi, M. Spira and P. M. Zerwas, Phys. Lett. B **264**, 440 (1991); S. Dawson, Nucl. Phys. B **359**, 283 (1991); D. Graudenz, M. Spira and P. M. Zerwas, Phys. Rev. Lett. **70**, 1372 (1993); M. Spira, A. Djouadi, D. Graudenz and P. M. Zerwas, Nucl. Phys. B **453**, 17 (1995) [hep-ph/9504378].
- [17] Z. Bern, L. J. Dixon and C. Schmidt, Phys. Rev. D **66**, 074018 (2002) [hep-ph/0206194].
- [18] Z. Bern, L. J. Dixon and D. A. Kosower, Phys. Rev. Lett. **70**, 2677 (1993) [hep-ph/9302280].
- [19] Z. Bern, L. J. Dixon and D. A. Kosower, Nucl. Phys. B **437**, 259 (1995) [hep-ph/9409393].
- [20] Z. Bern, A. De Freitas and L. J. Dixon, JHEP **0109**, 037 (2001) [hep-ph/0109078].
- [21] S. Catani and M. H. Seymour, Nucl. Phys. B **485**, 291 (1997) [Erratum-ibid. B **510**, 503 (1998)] [hep-ph/9605323].
- [22] T. Gleisberg and F. Krauss, Eur. Phys. J. C **53**, 501 (2008) [arXiv:0709.2881 [hep-ph]].
- [23] J. Ellis and T. You, arXiv:1303.3879 [hep-ph].
- [24] A. Djouadi, J. Kalinowski and M. Spira, Comput. Phys. Commun. **108**, 56 (1998) [hep-ph/9704448].
- [25] A. D. Martin, W. J. Stirling, R. S. Thorne and G. Watt, Eur. Phys. J. C **63**, 189 (2009) [arXiv:0901.0002 [hep-ph]].
- [26] N. Kauer and G. Passarino, JHEP **1208**, 116 (2012) [arXiv:1206.4803 [hep-ph]].